Electronic Supplementary Material (ESI) for MedChemComm.

Supplementary Information for

Neuroprotective Effect of Single-Wall Carbon Nanotubes with Built-In Peroxidase-Like Activity against β-Amyloid-Induced Neurotoxicity

Jeaha Shin [a], Sujin Lee [b], Misun Cha [*a,c]

[a]*Biotechnology Institute, Medifab Co. LTD., 70, Dusan-ro, Doksan-dong, Geumcheon-gu, Seoul, 085-84, South Korea.*

[b]*School of Mechanical and Aerospace Engineering, Seoul National University, 1 Gwanak-ro, Gwanak-gu, Seoul, Republic of Korea*

[c]*SMG-SNU Boramae Medical Center, 39 Boramae Gil, Dongjak-Gu, Seoul, 156-707, South Korea.*

*Address correspondence to: Misun Cha, Fax:+82-2-2181-3659; Tel: +82-2-2181-3658; E-mail:cmsbestok@gmail.com

EDS results of fSWNTs

After functionalize the SWNTs, SEM-EDX analysis confirmed that most metal catalysts such as Ni, Co, and Fe disappeared in the f-SWNTs.

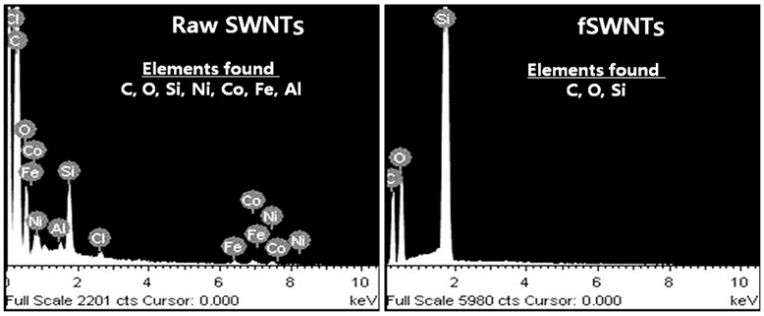

Fig. S1 EDS results of f-SWNTs. No impurities such as Ni, Co, Fe, and Al were detected in the fSWNTs.

BMP extraction and purification

BMPs were obtained from *Magnetospirillum* sp. AMB-1 (ATCC® 700264) that was cultured in magnetic spirillum growth medium (MSGM) for 5 days in a shaking incubator at 30 °C under anaerobic conditions. Cultured *Magnetospirillum* sp. AMB-1 were centrifuged for 25 min at 5,000 rpm and then lysed by sonicating (VCX500, Sonics & Materials, USA) for 30 min. BMPs were collected using a neodymium-iron-boron (NdFeB) magnet and then washed 5 times with 1X PBS. The collected BMPs were dispersed in 1X PBS and sterilized by autoclaving (121 °C, 15 min). The concentration of the extracted BMPs was determined using an inductively coupled plasma-atomic emission spectrometer (ICP-AEX, ICPS-7500, Shimadzu, Japan).

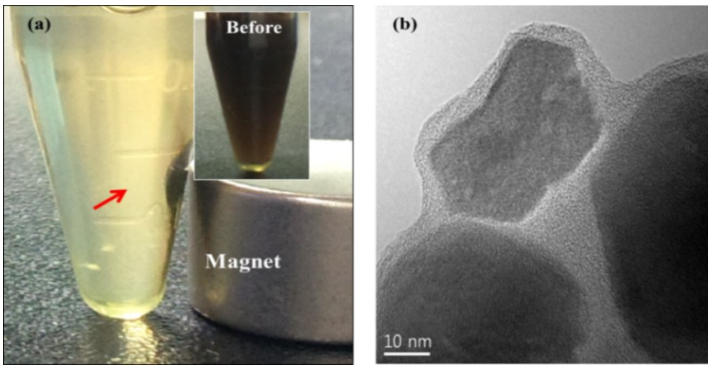

Fig. S2 (a) Magnetic attraction of BMPs, (b) TEM image of BMPs. Scale bar is 10 nm. The BMPs from the *Magnetospirillum* sp. AMB-1 used in our approach are inherently biocompatible, can be effectively conjugated with other biomolecules, and disperse well in aqueous solutions because of the stable lipid membranes surrounding their magnetic cores.

Conjugation of f-SWNTs to BMPs

The morphologies of the f-SWNT-BMP hybrids were analyzed using a high-resolution transmission electron microscope (HR-TEM; JEM-3000F, JEOL, Japan) and energy dispersive X-ray spectroscopy (EDS) analysis performed using a field-emission scanning electron microscope (FE-SEM; SUPRA 55VP, Carl Zeiss, Germany) with an X-ray microanalysis instrument

The morphological features of the hybrids significantly differed from those of the f-SWNTs with a clean surface. As shown in Fig. S2(a) and (d), elongated nanoparticles with spatially isolated features uniformly decorated the surfaces of individual f-SWNTs and/or small f-SWNT bundles. Furthermore, these elongated BMPs were mostly aligned on the nanotubes, although some exceptions were also observed.

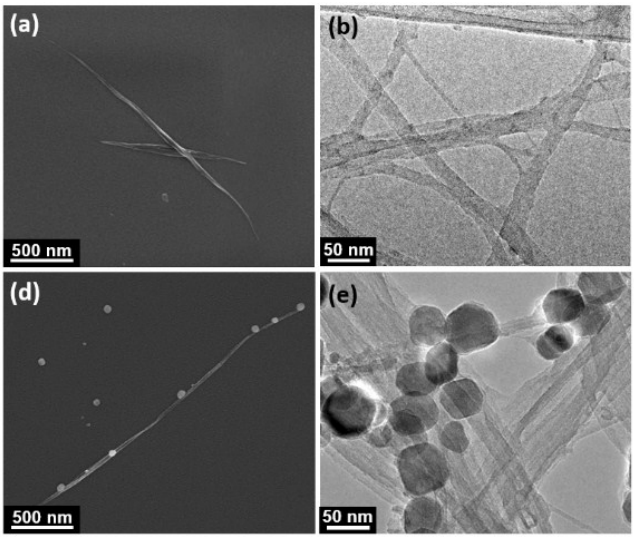

Fig. S3 Micrograph of f-SWNTs and f-SWNT-BMP hybrids (a), (b), (d), and (e). BMPs dangle from the f-SWNT bundles in the hybrid images (d) and (e), whereas only f-SWNTs are seen in images (a) and (b).

Binding properties of f-SWNTs to BMPs

Binding properties of BMP-SWNTs hybrid were confirm with raman spectroscopy and XPS analysis. Raman spectra were collected using a LabRam Aramis (Horiba Jobin-Yvon, France) spectrometer with an Ar-ion laser (514.532 nm) excitation source. A drop of each sample was loaded onto clean glass wafers and dried before analysis. Samples were focused using an optical microscope with a spot size of approximately 1 μm. The excitation power was 1 mW, and the spectra were calibrated prior to acquisition using a glass wafer. X-ray photoelectron spectroscopy (XPS) measurements were performed using a K-Alpha (Thermo Scientific) system. A drop of each sample was placed on a cleaned silicon wafer and dried in an oven at 70 °C overnight. A Kα

aluminum (1486.6 eV) X-ray source was used with a beam diameter of approximately 400 μm. The spectrometer energy was calibrated to the 3d5/2 electronic level of silver (368.2 eV) and the 2p3/2 electronic level of copper (932.8 eV). Low pressure in the sample chamber (6.5×10^{-9} mbar) was used for the analysis.

Figure S3(a) shows the Raman spectra for the unmodified SWNTs, f-SWNTs, and f-SWNT-BMP hybrids used to identify the characteristic peaks. When the unmodified SWNTs were compared with the f-SWNTs, the intensity of the G peak for the f-SWNTs and the hybrids showed no noticeable change; however, the intensity of the D peak was enhanced drastically, resulting in an increased intensity ratio of the D to G band (I_D/I_G). The D-band intensity measures the amount of sp^3 defects introduced by covalent addend binding; in general, a covalent attachment would lead to a drastic increase in the D-peak intensity [1]. For the f-SWNTs, the D/G ratio significantly increased, which was attributed to the generation of carboxyl and hydroxyl groups during the treatment process [1]. These results suggest that the route described here is a desirable approach for covalently attaching BMPs to the side walls; EDS/FE–SEM analysis confirmed the conjugation of BMPs onto the f-SWNT surface with C, O, and Fe on the surfaces of the hybrids (Fig. S3(b)). The Fe signals would have originated from the BMPs because most impurities, including Ni, Co, and Fe, that had been used as catalysts during the synthesis of the f-SWNTs were removed during the functionalization process (Fig. S3(c)). These results were further confirmed with XPS analysis. The expanded spectra of Fe 2p in Fig. S4(a) show the characteristic binding energy peaks of Fe 2p3/2 and Fe 2p1/2 of Fe_3O_4 [2]. As shown in Fig. 4S(b), the 400.1 eV peak was assigned to the residual amino groups on the surface of the Fe_3O_4, and the 401.0 eV peak was assigned to the amide groups in the hybrids [3].

References

1. Cançado, L. G.; Jorio, A.; Ferreira, E. H.; Stavale, F.; Achete, C. A.; Capaz, R. B.; Moutinho, M. V. O.; Lombardo, A.; Kulmala, T. S.; Ferrari, A. C. Nano Lett. 2011, ***11(8)****, 3190–3196.*

2. Correa-Duarte, M. A.; Grzelczak, M.; Salgueiriño-Maceira, V.; Giersig, M.; Liz-Marzan, L. M.; Farle, M.; Sierazdki, K.; Diaz, R. J. Phys. Chem. B 2005, ***109(41)****, 19060–19063.*

3. Liao, M. H.; Chen, D. H. J. Mater. Chem. 2002, ***12****, 3654–3659.*

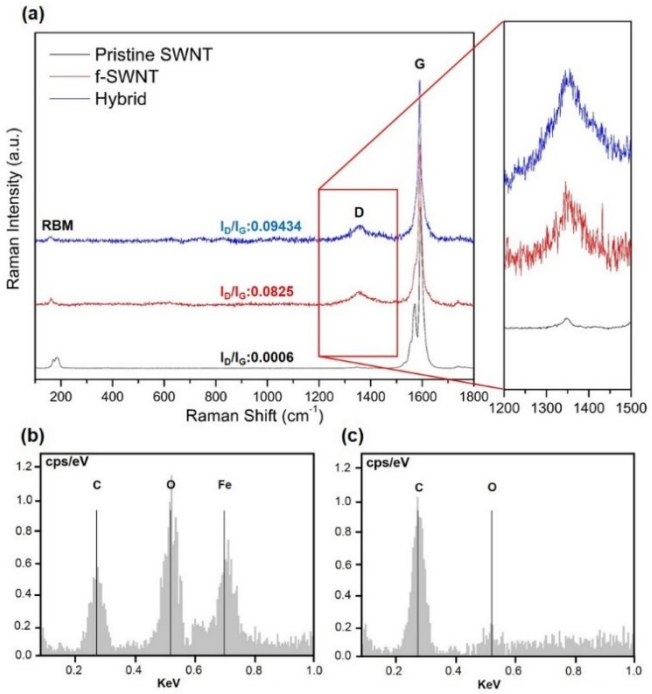

Fig. S4 Raman spectra (a), EDS results of f-SWNT-BMP hybrids (b) and f-SWNTs (c).When the unmodified SWNTs (pristine) were compared with the f-SWNTs, the intensity of the G peak for the f-SWNTs and the hybrids showed no noticeable change; however, the intensity of the D peak increased drastically, resulting in an increased intensity ratio of the D to G band (a). Inset: Starting from the bottom, the D peak of pristine SWNT, f-SWNT, and hybrid. The Fe signals would have originated from the BMPs (b) because most impurities, including Ni, Co, and Fe, that were used as catalysts during the synthesis of the f-SWNTs were removed during the functionalization process (c).

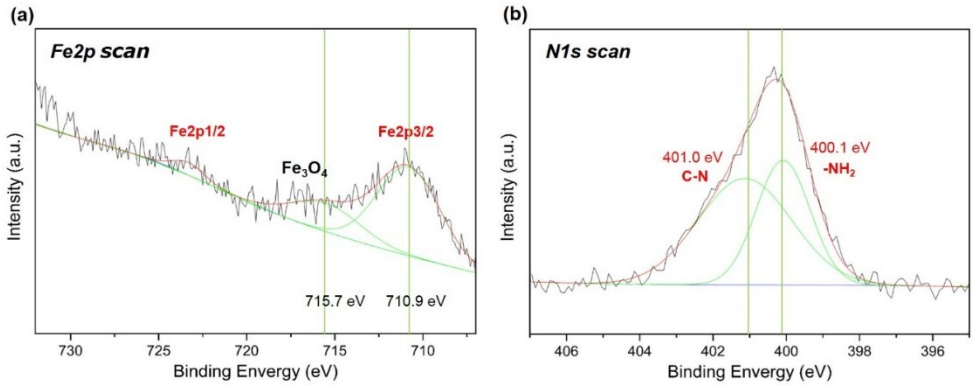

Fig. S5 XPS analysis of the Fe2p peak and the N1s core level of the hybrids. Fe2p scan showing the characteristic binding energy peaks of Fe 2p3/2 and Fe 2p1/2 of Fe_3O_4 (a). In the N1s scan, the 400.1 eV peak was assigned to the residual amino groups on the surface of Fe_3O_4, and the 401.0 eV peak was assigned to the amide groups in the hybrids (b).

Catalytic activity of f-SWNT-BMP hybrids

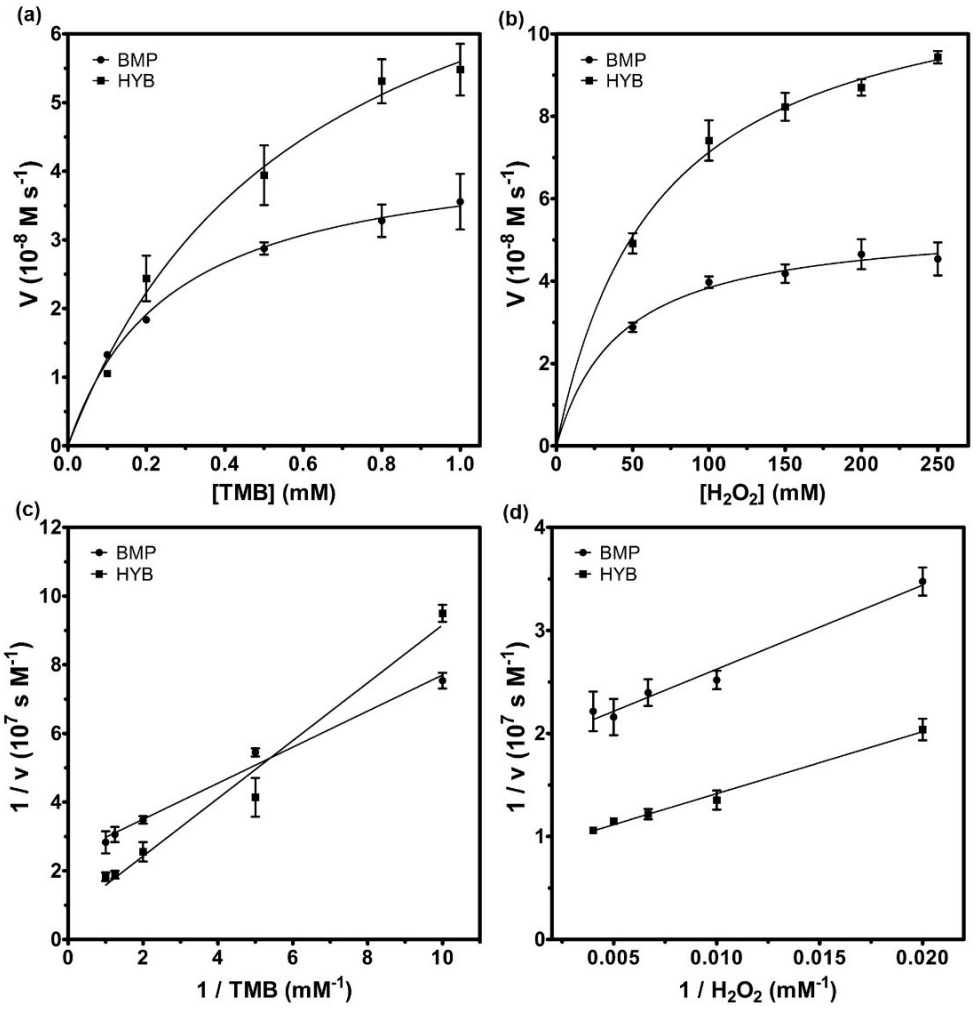

Fig. S6 Steady-state kinetic assay and catalytic mechanism of hybrids and BMPs. The concentration of H_2O_2 was 50 mM, and the TMB concentration varied (a). The concentration of TMB was 1.6 mM, and the H_2O_2 concentration varied (b). Double reciprocal plots of the activity of the hybrids and BMPs with a fixed concentration of H_2O_2 and varied TMB concentrations (c) and with a fixed concentration of TMB and varied H_2O_2 concentrations (d).

Table S1 Comparison of the apparent Michaelis–Menten constant (K_m) and maximum reaction rate (V_{max}) between hybrids and BMPs

	Km [mM]		Vmax [10^{-8} M s^{-1}]	
Catalyst	TMB	H2O2	TMB	H2O2
BMP	0.26±0.04	42.1±7.6	4.4±0.23	5.4±0.24

HYB	0.60±0.13	66.5±6.9	8.9±0.96	11.8±0.39

Interference of ThT fuorescence by fSWNTs, BMPs and BMP-SWNT hybrids

A measured fluorescence intensity is indicative of amyloid fibrils. In case of 100 μM Aβ, fluorescence intensity was increased almost twice after 48 hours compared to 3 hours result. We tested possible interference of ThT fuorescence by fSWNTs, BMPs and BMP-SWNT hybrids. In the presence of 10 μg/mL of SWNTs, 0.5 μg/mL of BMPs, or 10 μg/mL of the f-SWNT-BMP hybrids (SWNT:BMP = 20:1) used for the investigation of the effect on the aggregation of Aβ peptides, the interference level was extremely low.

To visualize Aβ fibrils, FITC-labeled Aβ antibodies were added to the samples after 7 days of Aβ peptide incubation in the presence and absence of the hybrids(Fig. S9(a)). Fig. S9 (b) shows a fluorescence image of the Aβ fibrils without hybrids, and it shows a strong signal compared with the Aβ fibril sample in the presence of hybrids (Fig. S9 (c)). And now we are preparing the next paper and our TEM data will be presented in that report.

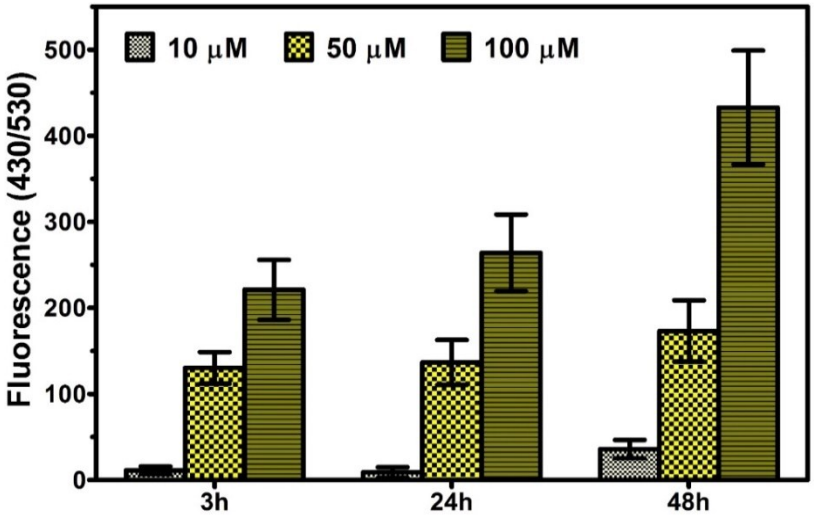

Fig. S7 Time dependent amyloid beta fibrillation with varying Aβ concentration

Table S2. Interference effect of by fSWNTs, BMPs and BMP-SWNT hybrids.

	Fluorescence (430/530), AVG(+STDV)		
	3h	24h	48h
fSWNTs	11.5(3.07)	13(3026)	11.75(4.78)
BMPs	5.5(3.81)	7(4.32)	6.75(2.87)
HYB	14(1.51)	12.75(4.19)	16.5(2.08)
100mM aβ	233(11.71)	311.25(15.30)	507.5(26.91)

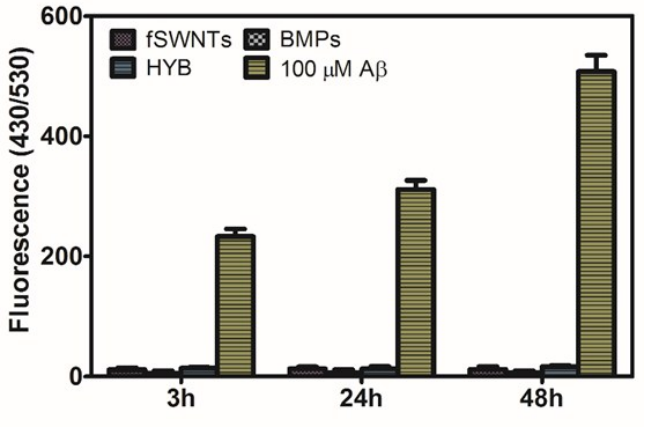

Fig. S8 Interference effect of by 10 μg/mL of SWNTs, 0.5 μg/mL of BMPs, or 10 μg/mL of the f-SWNT-BMP hybrids (SWNT:BMP = 20:1)

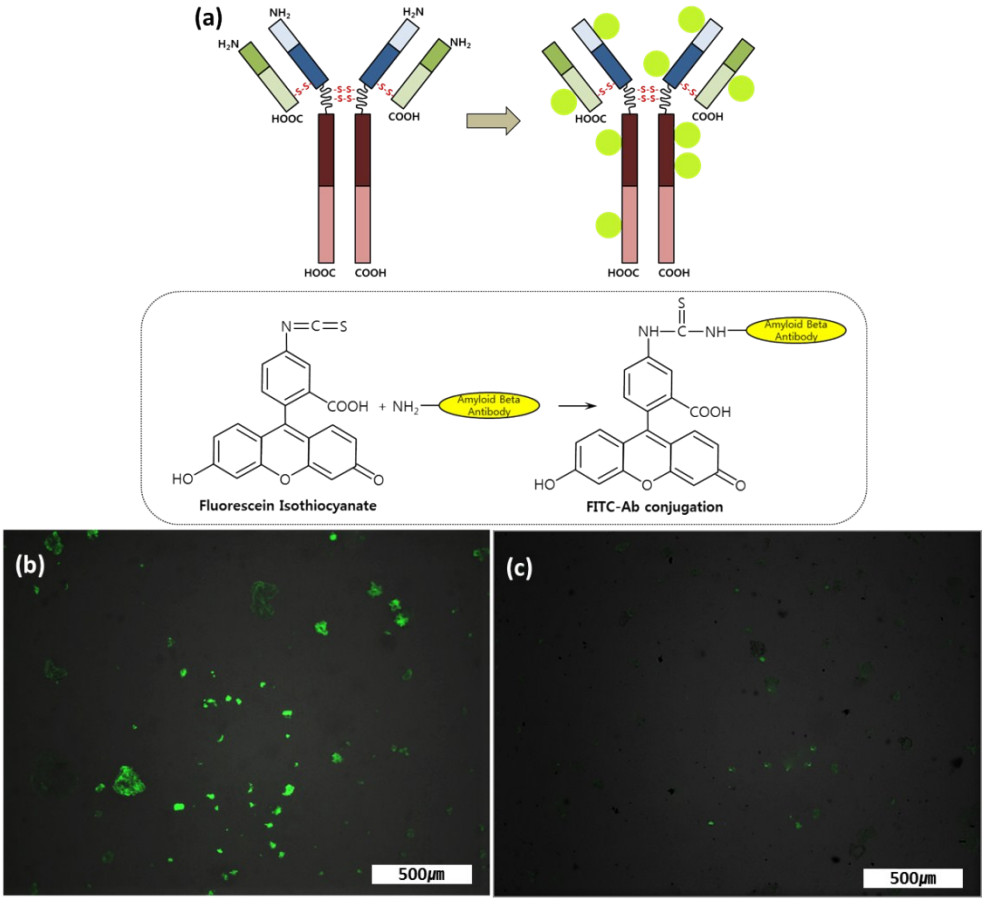

Fig. S9 Fluorescence images of Aβ fibrils in the absence and presence of hybrids. (a) Amyloid Beta antibody-FITC conjugation. A fluorescence image of Aβ without (b) and with (c) Hybrid. To visualize Aβ fibrils in solution, FITC-labeled Aβ antibodies were combined with the samples after 7 days of Aβ incubation. A fluorescence image of Aβ without hybrids (b) shows a stronger signal than the Aβ with hybrids (c).

Effect of amyloid-beta fibrillation inhibition

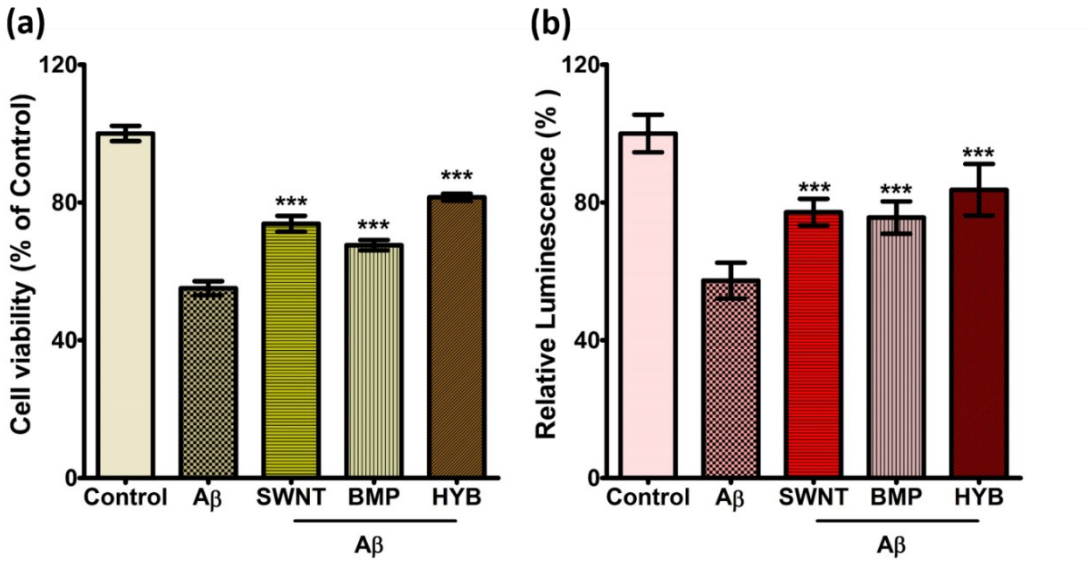

Fig. S10 SH-SY5Y cell viability increases due to amyloid-beta fibrillation inhibition by various nanoparticles. MTS assay result (a) and ATP assay result (b). 0.01 μg/mL of single-walled carbon nanotubes(SWNT), 0.005 μg/mL of bacterial magnetic nanoparticles(BMP), and 0.01 μg/mL of SWNT-BMP hybrids(HYB) was mixed with 200 μM of 25-35 amyloid beta(Aβ) to inhibit its fibrillation. For comparison, Aβ without nanoparticle is also treated into the cells and incubated for 3 days to generate Aβ fibril induced neurotoxic condition (Control). SWNT and BMP treated cells showed about 20 % of cell viability increase compared to Aβ injured cells. Both MTS and ATP assay result showed that cell viability of hybrid treated cell increased more than 30 %. (***$p<0.001$ compared to Aβ treated cell, n=6)